

SUPPLEMENTARY INFORMATION *for*

Observation of Multiple Charge Density Wave Phases in Epitaxial

Monolayer 1T-VSe₂ Film

Junyu Zong, Yang Xie, Qinghao Meng, Qichao Tian, Wang Chen, Xuedong Xie,
Shaoen Jin, Yongheng Zhang, Li Wang, Wei Ren, Jian Chen, Aixi Chen, Fang-Sen
Li, Zhaoyang Dong, Can Wang, Jian-Xin Li, Yi Zhang

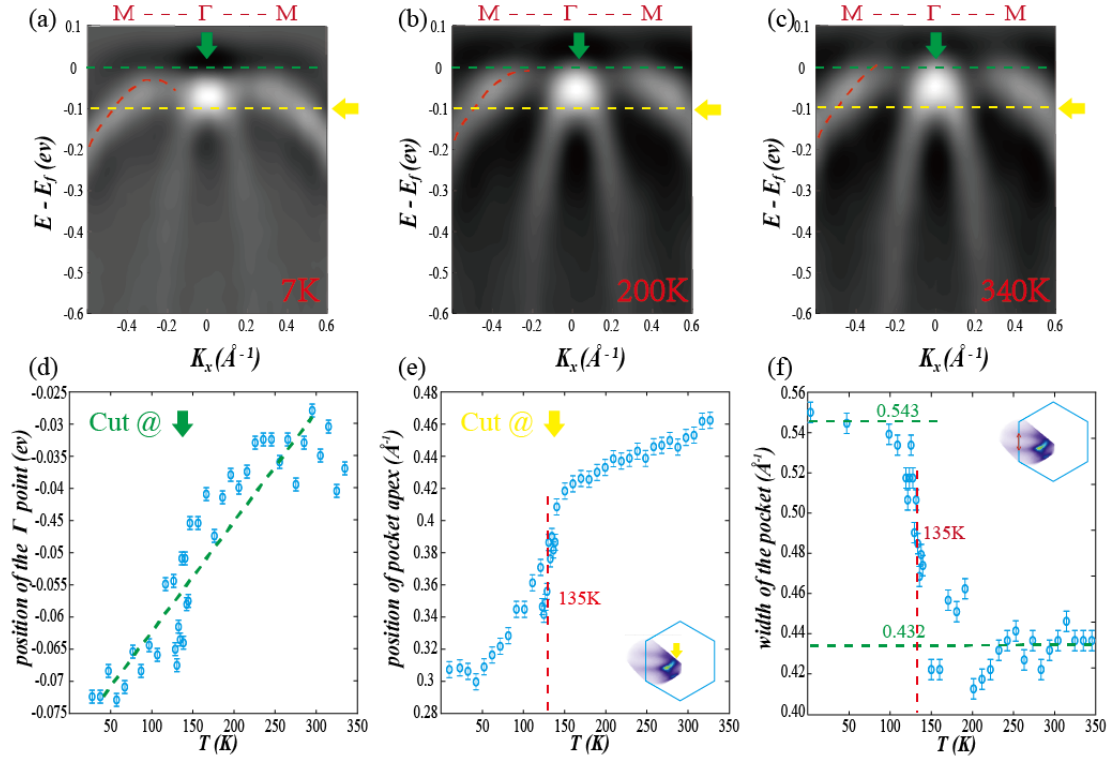
A: Methods

The growth and measurements of the 2D 1T-VSe₂ films were performed in a combined MBE-STM-ARPES ultra-high vacuum (UHV) system with a base pressure of $\sim 2 \times 10^{-10}$ mbar. The substrate bilayer graphene (BLG) was obtained by flash-annealing the 4H-SiC (0001) wafer to ~ 1250 °C. The V flux was produced from high-temperature heating evaporator. The high purity Se (99.9995%) was evaporated from a standard Knudsen cell. The BLG substrate was kept at 280 °C during the growth. The surface morphology was measured by the *in-situ* RHEED and STM at room temperature. The XPS and ARPES measurements were performed via a Scienta Omicron DA30L analyzer. The monochromatic X-ray (SIGMA) was generated from an Al electrode excitation source (Al _{α} , 1486.7 eV), and the ultraviolet (UV) light source was generated by a Helium lamp (Fermi Instruments) with a SPECS monochromator (He I, 21.218 eV). The samples were cooled down to ~ 7 K by a close-cycle cryogenerator during the measurements, and the sample temperature can be controlled by an *in-situ* inner heater in the manipulator. The first-principles calculations were performed using the QUANTUM ESPRESSO package based on density functional theory (DFT). The generalized gradient approximation with the Perdew-Burke-Ernzerhof functional was used to describe the electron exchange and correlation effects. A plane-wave energy cutoff of 80 Ry and a $16 \times 16 \times 1$ k mesh was employed. Freestanding films were modeled with a 23 Å vacuum gap between adjacent layers in

the supercell. The in-plane lattice parameter was fixed to the experimentally reported value of 3.35 Å. Structures were fully optimized until ionic forces and energy difference are less than 10^{-3} eV/Å and 10^{-5} eV.

B: Temperature Dependence of the Fermi surface

To better understand the mechanism of CDW in monolayer 1T-VSe₂, we further study the secondary differential spectra along the $M-\Gamma-M$ direction [Figures S1(a)-S1(c)]. The bent band marked by the red dashed line will straighten gradually until it finally crosses the Fermi level with increasing temperature. We plot the trend of the width of oval pockets around the M points at the boundary of BZ [shown by the red arrow in the upper right inset of Figure S1(f)] with various temperatures in Figure S1(f). The pocket width decreases from 0.543 Å⁻¹ to 0.432 Å⁻¹ at the transition temperature of 135 K (red dashed line), indicating that the oval pocket has been shrinking as temperature increases. Immediately afterwards, we get the temperature dependence of the position of oval pocket apex in Figure S1(e) [along the yellow dashed lines in Figures S1(a)-S1(c)]. The position of the oval pocket apex [shown by the lower right inset of Figure S1(e)] in momentum space moves away from the Γ point from 0.3 Å⁻¹ to 0.46 Å⁻¹ as temperature increases. Notably, a mutation can be observed at 135 K (marked by the red dashed line), and the position of oval pocket apex will still move slowly away from Γ point after 150 K. It is different from the change of the oval pocket width, which hardly shrinks after 150 K. To determine whether it is a shrinkage or a movement of the pocket apex caused by the raise of the tapered band at the Γ point. We analyze the top of the tapered band at the Γ point [Figure S1(d)]. During temperature increases, the top of the tapered band at the Γ point raises linearly from -0.075 eV to -0.028 eV below the Fermi level. Therefore, it squeezes the pocket apex away from the Γ point, but the width of the oval pocket will not shrink after 150K. Thus, we suggest that this shrinkage of the oval pockets around M points fails the near Fermi nesting wave vectors and $(\sqrt{7}\times\sqrt{3})$ CDW phase completely disappears after 135 K.



S1. Fermi surface evolution with the increasing temperature. (a)-(c) The secondary differential spectra along the $M-\Gamma-M$ direction at 7 K, 200 K, and 340 K respectively. (d) The analysis of the top of the tapered band at the Γ point indicated by the green arrow in (a)-(c). (e) The temperature dependence of the momentum position of the pocket apex which cut along the yellow dashed lines marked by the yellow arrow in (a)-(c). The position of the pocket vertex is shown in the lower right inset. (f) The temperature dependence of the width of oval pocket around the M point at the boundary of the BZ (shown by the red double arrow in the upper right inset).